Supporting Information for "Quantifying nitrous oxide emissions in the U.S. Midwest - A top-down study using high resolution airborne in-situ observations"

Maximilian Eckl[1], Anke Roiger[1], Julian Kostinek[1], Alina Fiehn[1], Heidi

Huntrieser[1], Christoph Knote[2], Zachary R. Barkley[3], Stephen M. Ogle[4],

Bianca C. Baier [5,6], Colm Sweeney[6], and Kenneth J. Davis[3,7]

[1]Deutsches Zentrum für Luft- und Raumfahrt (DLR), Institut für Physik der Atmosphäre, Oberpfaffenhofen, Germany

[2]Ludwig-Maximilians-University (LMU), Meteorological Institute, Munich, Germany

[3]Department of Meteorology and Atmospheric Science, Pennsylvania State University, University Park, PA, USA

[4]Natural Resource Ecology Laboratory, Colorado State University, Fort Collins, CO, USA

[5]Cooperative Institute for Research in Environmental Sciences, University of Colorado-Boulder, Boulder, CO, USA

[6]NOAA Global Monitoring Laboratory, Boulder, CO, USA

[7]Earth and Environmental Systems Institute, Pennsylvania State University, University Park, PA, USA

―――――――

Corresponding author: M. Eckl, Institut für Physik der Atmosphäre, Deutsches Zentrum für Luft- und Raumfahrt (DLR), Münchener Straße 20, 82234 Weßling, Germany. (Maximilian.Eckl@dlr.de)

October 14, 2020, 3:27pm

Contents of this file

1. Text S1 to S5

2. Figure S1 to S3

3. Tables S1 to S3

Introduction

Here we provide additional information on the employed model setup (Text S1), the EDGAR sectors (Text S2 and Table S1), the linear relationship between the tracer integral along a transect and the emission strength (Text S3 and Table S2), the uncertainties in the Monte Carlo simulations (Text S4), the influence of the bias correction on the results (Text S5 and Table S3), the background (Figure S1), and the model performance (Figure S2 and S3).

Text S1: Model setup

Simulations are performed with WRF-Chem version 4.0.2. The employed model physics configuration includes the Thompson scheme for microphysics, RRTMG for radiation, Kain-Fritsch for cumulus parameterization, MYNN 2.5 level TKE for PBL physics and the Noah land-surface model. Vertically, each domain encompasses 50 terrain-following layers, with a greater resolution near the ground. Two-way nesting enables information transfer between the domains. Moreover, we use the WRF Four Dimensional Data Assimilation (FDDA) feature to perform analysis nudging in the outer domain, to ensure an optimal meteorological model solution.

Text S2: EDGAR sector description

We merge the different EDGAR sectors into three main sectors: Agricultural E_{AGR}, non-agricultural anthropogenic E_{nonAGR}, and natural emissions E_N. E_{AGR} covers emissions from agricultural soils, indirect emissions from agricultural soils, manure management,

and agricultural waste burning, whereas E_{nonAGR} consists of all remaining anthropogenic

EDGAR sectors, including (among others) road transportation, chemical processes, and

power industry. E_N encompasses natural soil and ocean emissions. As emissions from

oceans did not contribute to Midwest N_2O enhancements in our simulations, our E_N in-

volves only natural soil emissions. The applied assumption that all those sources originate

from the surface is valid except for aviation related emissions. Since those account for

less than $0.3\,\%$ of the yearly total EDGAR Midwest emissions, we excluded them from

E_{nonAGR} under the assumption that this would not have a significant impact on our results.

A detailed listing of all EDGAR sectors can be found in Table S1.

Text S3: Linearity of tracer integral and emission strength

For each flight the area summed agricultural emissions E_{AGR}^{sum} are linear to the correspond-

ing tracer integral along a transect A_{AGR}. This implies that if agricultural emissions are

scaled by a certain factor, the tracer integral is also scaled by this factor. To verify this, we

simulated each flight day with a E_{AGR} multiplied by 10, 20, and 30 (F_{AGR}^E) and compared

those factors with the resulting magnitude of enlargement in A_{AGR} (F_{AGR}^A). A linear re-

gression between F_{AGR}^E and F_{AGR}^A (see Table S2) exhibits negligible residuals and a slope

and y-intercept which differs insignificantly from one and zero, respectively, proving the

equivalence of F_{AGR}^E and F_{AGR}^A.

Text S4: Uncertainties in Monte Carlo simulation

The uncertainties of the observed background ($\sigma = \pm 0.5\,\mathrm{ppb}$ and $\sigma = \pm 0.9\,\mathrm{ppb}$ for 2017

and 2019, respectively) are the standard deviation of all 2nd low level leg percentiles of a whole campaign. The background uncertainties are dominated by large scale circulations and long term variability such as seasons, and are probably not normally distributed. However, too few observations prevent the determination of the actual distribution. Here, we assume that a normal distribution is the best first order guess. Janssens-Maenhout et al. (2019) states the relative 1σ uncertainty of total EDGAR4.3.2 N_2O emissions in the U.S. to be 21%. No sector-specific uncertainty is provided. Hence, we use this value as a rough estimate for the uncertainty of only non agricultural emissions. As we could not find uncertainty estimates for EDGAR5.0 and EDGAR2 we assume them to be the same and twice as in EDGAR4.3.2, respectively. For days with large agricultural correction factors F_{AGR} the uncertainties of E_{nonAGR} and E_N affect the results only marginally. Hence, this uncertainty analysis is implicitly based on the assumption that E_{nonAGR} and E_N are well represented in the inventories compared to E_{AGR}. Following Butterbach-Bahl, Baggs, Dannenmann, Kiese, and Zechmeister-Boltenstern (2013) mainly N_2O emissions from soils account for the uncertainty in N_2O budgets on regional and national scales, which supports our assumption.

Text S5: Bias correction

Following Barkley et al. (2019), the bias due to an erroneous modeled wind speed and PBL height can be corrected with:

$$C_{mod}^{corr} = C_{mod} \cdot \frac{U_{mod} \cdot Z_{mod}}{U_{obs} \cdot Z_{obs}} \tag{1}$$

Here, C_{mod} is the modeled N$_2$O enhancement along a transect and C_{mod}^{corr} the corresponding bias corrected one, which is further used for the model optimization. U_{mod}/U_{obs} is the modeled/observed wind speed averaged along the transect. For the observed PBL height Z_{obs} we use in situ soundings conducted with the C-130 at the beginning, the end, and during the transect. For each flown sounding the PBL height is determined as the lowest (regarding altitude) significant maximum of the observed virtual potential temperature lapse rate profile. The average of all determined PBL heights defines Z_{obs} of the transect. For the modeled PBL height of a transect Z_{mod} we use the modeled profiles at the grid points closest to the flown soundings and perform the same approach as for Z_{obs}. However, there is a caveat here. We correct for model errors at the position of the aircraft at a certain time but we are simulating large areas for several days. The model error varies over space and time, thus, limiting the benefit of the posed bias correction. Table S3 summarizes the results of the bias correction.
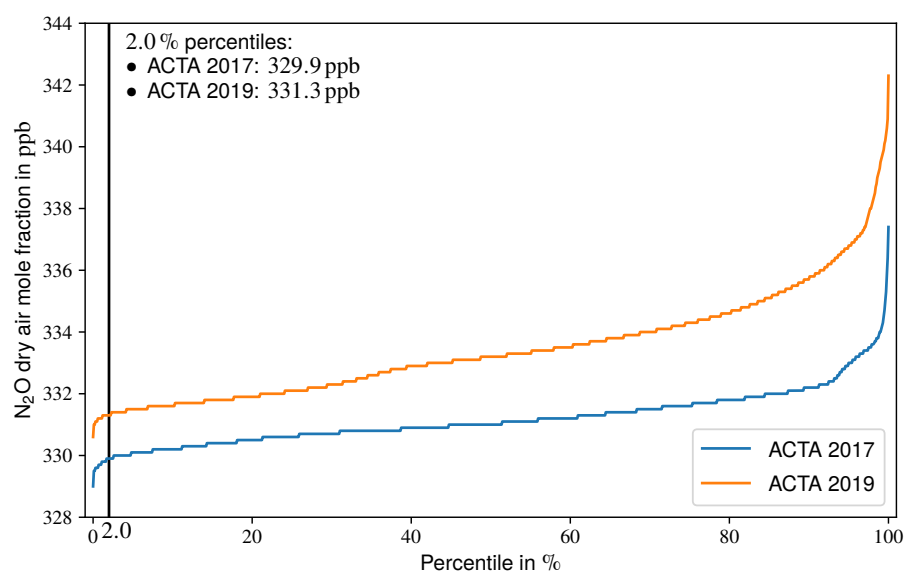
Figure S1. Percentiles for ACTA 2017 and ACTA 2019. Low level legs (at approx. 1000 ft AGL) of all conducted flights were merged and the corresponding percentiles were calculated.
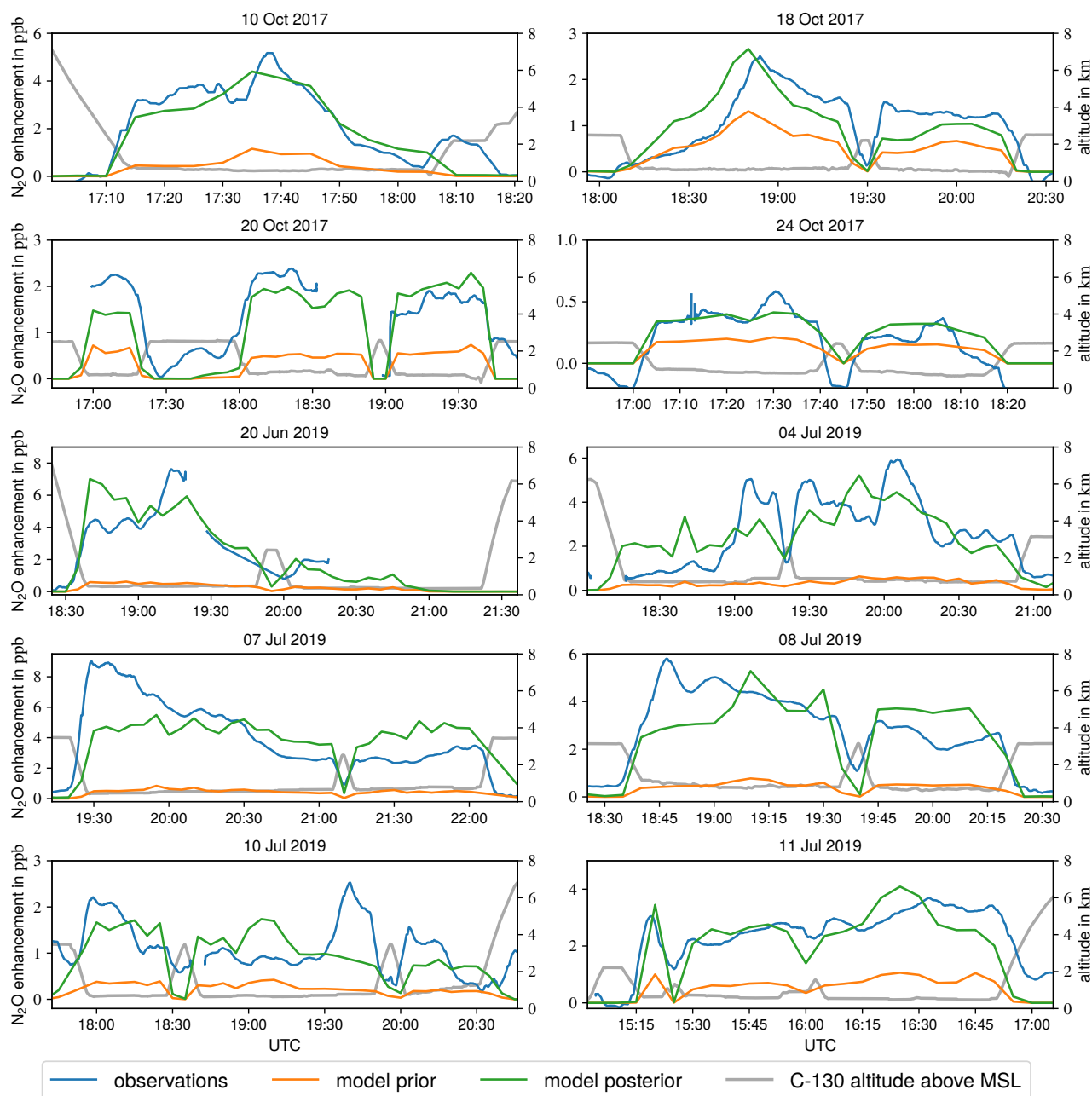
Figure S2.   Observed vs. modeled N$_2$O enhancement (emitted from EDGAR4.3.2/EDGAR2 $E_{AGR} + E_{nonAGR} + E_N$) for each of the ten investigated flights. For an easier visual comparison the 5 min-moving average of the observations is shown. The modeled enhancements are the mean from the three model runs with different initial and boundary meteorological conditions (ERA5, GDAS-FNL, and NARR) on the closest grid points in space and time to each observation.
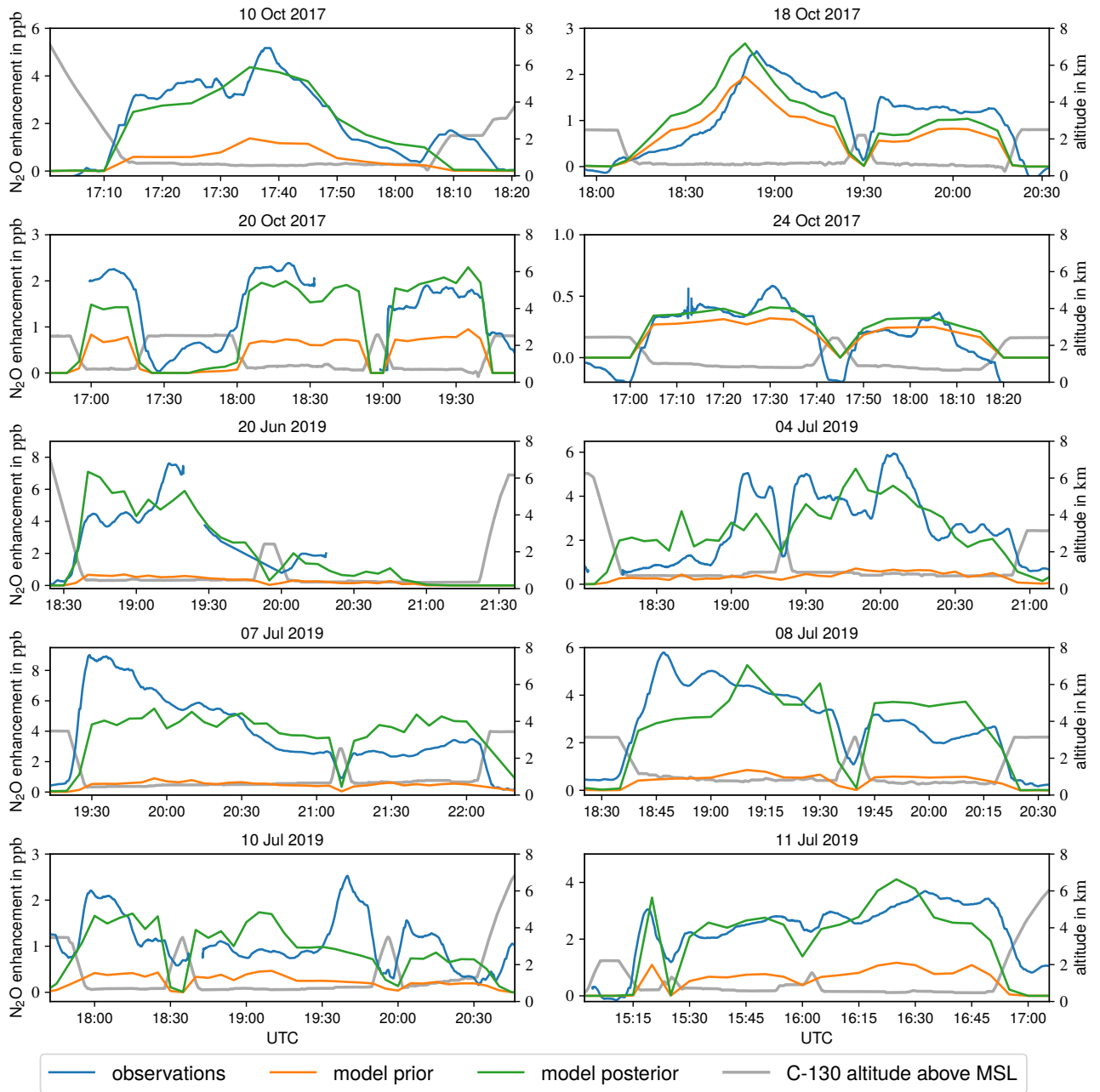
October 14, 2020, 3:27pm

Figure S3. As Figure S2 but modeled N$_2$O enhancement emitted from EDGAR5.0/EDGAR2

$E_{AGR} + E_{nonAGR} + E_N$.

Table S1.   Components of E_{AGR}, E_{nonAGR}, and E_N. If not otherwise specified, sectors are included in EDGAR4.3.2 and EDGAR5.0. All existing EDGAR4.3.2/EDGAR5.0 N_2O sectors are listed as well as all natural EDGAR2 sectors.

main sector	EDGAR sector	IPCC (2006b) code
E_{AGR}	Manure management	3A2
	Agricultural waste burning	3C1b
	Agricultural soils	3C2+3C3+3C4+3C7
	Indirect N_2O emissions from agriculture	3C5+3C6
E_{nonAGR}	Power industry	1A1a
	Oil refineries and transformation industry	1A1b+1A1ci+1A1cii+1A5biii+1B1b+1B2aiii6+1B2biii3+1B1c
	Combustion for manufacturing	1A2
	Road transportation	1A3b
	Railways, pipelines, off-road transport	1A3c+1A3e
	Shipping	1A3d
	Energy for buildings	1A4+1A5
	Fuel exploitation	1B1a+1B2aiii2+1B2aiii3+1B2bi+1B2bii
	Chemical processes	2B
	Solvents and products use	2D3+2E+2F+2G
	Solid waste landfills	4A+4B
	Solid waste incineration	4C
	Waste water handling	4D
	Indirect emissions from NO_x and NH_3	5A
	Fossil fuel fires	5B
E_N	Natural soils (just EDGAR2)	–
excluded	Aviation climbing and descent	1A3a_CDS
	Aviation cruise	1A3a_CRS
	Aviation landing and takeoff	1A3a_LTO
	Aviation supersonic	1A3a_SPS
	Oceans (just EDGAR2)	–

Table S2. Results of a linear regression between F_{AGR}^E and F_{AGR}^A and their correlation R. Every flight day was simulated with a F_{AGR}^E of 10, 20, and 30 and the corresponding F_{AGR}^A was calculated. The regression was performed via a least squares polynomial fit. The residual is the squared Euclidean 2-norm. See Text S3 for a description of F_{AGR}^E and F_{AGR}^A.

EDGAR version	slope	slope-1	y-intercept	residual	R	R-1
v4.3.2	1.0	-0.05×10^{-3}	-0.47×10^{-3}	0.02×10^{-3}	1.0	-0.02×10^{-7}
v5.0	1.0	1.28×10^{-3}	-1.26×10^{-3}	3.39×10^{-3}	1.0	-3.6×10^{-7}

Table S3.   Modeled vs. observed wind speed and PBL height for each flight and the corresponding bias correction factor. In the model columns the first value belongs to the ERA5, the second to the GDAS-FNL, and the third to the NARR simulation.

Day	U_{obs} in $\mathrm{m\,s^{-1}}$	U_{mod} in $\mathrm{m\,s^{-1}}$	$\frac{U_{mod}}{U_{obs}}$	Z_{obs} in m	Z_{mod} in m	$\frac{Z_{obs}}{Z_{mod}}$	$\frac{U_{mod}\cdot Z_{mod}}{U_{obs}\cdot Z_{obs}}$
10 Oct 2017	3.5	5.2 3.0 3.7	1.5 0.9 1.1	1067	1134 1319 1325	1.1 1.2 1.2	1.6 1.1 1.3
18 Oct 2017	10.6	12.9 12.9 12.8	1.2 1.2 1.2	1417	1106 1307 1116	0.8 0.9 0.8	0.9 1.1 1.0
20 Oct 2017	13.1	17.9 17.3 17.2	1.4 1.3 1.3	1273	963 1013 1084	0.8 0.8 0.9	1.0 1.1 1.1
24 Oct 2017	15.7	15.9 15.9 15.5	1.0 1.0 1.0	1603	1565 1716 1668	1.0 1.1 1.0	1.0 1.1 1.0
20 Jun 2019	7.1	9.1 9.0 8.4	1.3 1.3 1.2	1480	1024 1188 1094	0.7 0.8 0.7	0.9 1.0 0.9
04 Jul 2019	4.9	5.1 4.3 3.5	1.0 0.9 0.7	1684	1784 1944 2080	1.1 1.2 1.2	1.1 1.0 0.9
07 Jul 2019	4.3	4.6 3.7 3.5	1.1 0.9 0.8	1889	2417 2420 2246	1.3 1.3 1.2	1.4 1.1 1.0
08 Jul 2019	9.0	10.2 10.1 9.3	1.1 1.1 1.0	1718	1955 2055 1994	1.1 1.2 1.2	1.3 1.3 1.2
10 Jul 2019	10.4	10.2 10.9 10.2	1.0 1.0 1.0	1767	1956 1893 2014	1.1 1.1 1.1	1.1 1.1 1.1
11 Jul 2019	6.7	7.3 5.8 6.6	1.1 0.9 1.0	1659	1861 1638 1608	1.1 1.0 1.0	1.2 0.9 1.0

References

Barkley, Z. R., Davis, K. J., Feng, S., Balashov, N., Fried, A., DiGangi, J., ... Halliday, H. S. (2019). Forward Modeling and Optimization of Methane Emissions in the South Central United States Using Aircraft Transects Across Frontal Boundaries. *Geophysical Research Letters*, *46*(22), 13564–13573. doi: 10.1029/2019gl084495

Butterbach-Bahl, K., Baggs, E. M., Dannenmann, M., Kiese, R., & Zechmeister-Boltenstern, S. (2013). Nitrous oxide emissions from soils: how well do we understand the processes and their controls? *Philosophical Transactions of the Royal Society B: Biological Sciences*, *368*, 20130122. doi: 10.1098/rstb.2013.0122

Janssens-Maenhout, G., Crippa, M., Guizzardi, D., Muntean, M., Schaaf, E., Dentener, F., ... Oreggioni, G. D. (2019). EDGAR v4.3.2 Global Atlas of the three major greenhouse gas emissions for the period 1970–2012. *Earth System Science Data*, *11*(3), 959–1002. doi: 10.5194/essd-11-959-2019